THE PHYSICAL REVIEW

A journal of experimental and theoretical physics established by E. L. Nichols in 1893

SECOND SERIES, VOL. 74, NO. 10 NOVEMBER 15, 1948

The Interaction of High Energy Neutrons and Heavy Nuclei

M. L. GOLDBERGER

Physics Department, University of Chicago, Chicago, Illinois

(Received July 20, 1948)

The interaction of high energy neutrons with heavy nuclei is studied under the assumption that the nucleus may be described by the statistical model. A detailed study is made of the energy transferred to the nucleus, the angular distribution of emerging particles, and the effective cross section for neutrons passing through nuclear matter. A summary of the results is given in the final section of the paper.

I. INTRODUCTION

THE 100-Mev neutrons produced by the Berkeley cyclotron[1] provide a powerful experimental tool for the study of the properties of heavy nuclei. Considerable work has already been done on the investigation of fission thresholds and nuclear reactions in heavy elements.[2] It is the purpose of this paper to investigate in detail the transfer of energy to the nucleus by high energy neutrons and to study the scattering of neutrons by heavy nuclei.

The general principles of high energy nuclear reactions have been described by Serber,[3] and the point of view presented by him will be adopted, for the most part, in this work. The main ideas enunciated by Serber are that one must consider individual nucleon-nucleon collisions in which a relatively small amount of energy is transferred on a single collision and that one must take into account the degeneracy of nuclear matter, i.e., effects due to the presence of nucleons other than the particular collision partner in question. This will be taken into account using the statistical model of the nucleus.[4] The experimentally measured neutron-proton cross section[5] will be used whenever possible, to characterize the individual collisions taking place inside the nucleus.

In Section II, the problem of the effective mean free path in nuclear matter is duscussed in conjunction with a preliminary calculation of the scattering of nucleons by heavy nuclei. In Section III the energy transferred to the nucleus is studied in detail and the number and energy distribution of particles emitted "immediately" after a collision is discussed. (It should be noted that the problems discussed will not be those concerning what happens to the energy transferred to the nucleus, the results of which are usually described by the evaporation model.[3, 6] The events of interest here are those which take place in the order 10^{-22} sec.) In Section IV the results are summarized and a discussion of the possibilities of experimental verification is given.

[1] Helmholz, McMillan, and Sewell, Phys. Rev. **72**, 1003 (1947).
[2] Cook, McMillan, Peterson, and Sewell, Phys. Rev. **72**, 1264 (1947).
[3] R. Serber, Phys. Rev. **72**, 1114 (1947).
[4] H. Bethe and R. Bacher, Rev. Mod. Phys. **8**, 83 (1936).
[5] Hadley, Kelly, Leith, Segrè, Wiegand, and York, Phys. Rev. **73**, 1114 (1948).
[6] P. Wolff and W. Heckrotte, Phys. Rev. **73**, 264 (1948).

II. THE EFFECTIVE MEAN FREE PATH IN NUCLEAR MATTER AND THE SCATTERING OF NEUTRONS BY HEAVY NUCLEI

A. The Mean Free Path

The first problem to be investigated is the mean free path of a nucleon when it is inside the nucleus. According to our model, we picture the nucleus as a mixture of two non-interacting, Fermi gases of neutrons and protons bound in a uniform potential of depth about 26 Mev, the highest filled state being at an energy of about -8 Mev. The maximum Fermi energies of the neutrons and protons are E_n and E_p, respectively, and are given by the well-known formula

$$E_F=(\hbar^2/2M)(3\pi^2N/V)^{\frac{2}{3}}, \quad (1)$$

where N is the number of neutrons or protons, V is the nuclear volume, and M is the mass of a nucleon. For simplicity, we shall assume that there is only one kind of particle inside the nucleus and use for the effective number of particles one-fourth the number of neutrons plus the number of protons. The reason for using only one-fourth the number of neutrons is that on the basis of an interaction consisting of one-half exchange and one-half ordinary forces which seems to be necessary to fit the observed neutron-proton scattering data[7] the total neutron-neutron cross section is about one-fourth the neutron-proton cross section. The exclusion principle will, however, be taken into account for the incident particle by demanding that the projectile as well as the target particle be outside the occupied sphere in momentum space after the collision. The radius of the sphere is given by

$$P=\hbar(3\pi^2N/V)^{\frac{1}{3}}. \quad (2)$$

It is easy to show that the most probable momentum transfer in a high energy nucleon-nucleon collision is of the order of $\hbar/r_0$, where r_0 is the range of nuclear forces. Since $\hbar/r_0P$ is of the order of $\frac{1}{2}$, a sizeable fraction of collisions are forbidden by the Pauli principle and thus the effective cross section is decreased. It is just this effect which will be computed.

Consider a neutron with energy E_0' incident upon a nucleus. Inside the nucleus it has an energy $E_0=E_0'+V_0$ where V_0 is the well depth. It will be convenient to measure all momenta in units of P and all energies in units of $P^2/2M$, and this will be done throughout the paper. Let the momentum of the incident neutron (inside the nucleus) be $\mathbf{P}_0$ and that of one of the target nucleons be $\mathbf{P}_1$. It will be assumed that the cross section for a collision between $\mathbf{P}_0$ and $\mathbf{P}_1$, namely, $\sigma d\Omega\mathbf{p}_f$, is known. Here $d\Omega\mathbf{p}_f$ is an element of solid angle about the final projectile momentum $\mathbf{p}_f$ in the center of mass frame of the two collision partners. Obviously $p_f=p_0=|\mathbf{P}_0-\mathbf{P}_1|/2$ where $\mathbf{p}_0$ is the initial momentum in the center of mass frame. In general σ is a function of p_0 and the angle between $\mathbf{p}_0$ and $\mathbf{p}_f$. No assumption of the precise dependence will be made at this point. For convenience of expressing results in the laboratory frame, it is expedient to replace the element of solid angle by a three-dimensional volume element in momentum space. Let the momentum transfer in a collision be $\mathbf{g}$ where $\mathbf{g}=\mathbf{p}_f-\mathbf{p}_0=\mathbf{P}_f-\mathbf{P}_0$ and $\mathbf{P}_f$ is the final projectile momentum in the laboratory frame. The volume element transformation is as follows:

$$\sigma d\Omega\mathbf{p}_f=\sigma\frac{1}{p_f^2}\delta(p_f-p_0)d\mathbf{p}_f=\sigma\frac{1}{p_0^2}\delta(p_f-p_0)d\mathbf{g}, \quad (3)$$

where the last writing follows from the definition of $\mathbf{g}$ if $\mathbf{P}_1$ is regarded as fixed. $\mathbf{p}_f$ and $\mathbf{p}_0$ are now assumed to be expressed as functions of $\mathbf{g}$ and $\mathbf{P}_1$. The effective total cross section $\bar{\sigma}$ is then found by integrating the product of the relative velocity $|\mathbf{P}_0-\mathbf{P}_1|/M$ and the cross section over the allowed regions of $\mathbf{P}_1$ and dividing by the incident velocity P_0/M:

$$\bar{\sigma}=\frac{1}{P_0}\int d\mathbf{g}\int d\mathbf{P}_1N(\mathbf{P}_1)|\mathbf{P}_0-\mathbf{P}_1| \times\sigma(p_0,\mathbf{p}_0\cdot\mathbf{p}_f)\frac{1}{p_0^2}\delta(p_0-p_f), \quad (4)$$

where $N(\mathbf{P}_1)$ is the density of target nucleons in momentum space. The allowed regions of integration are confined to those values of $\mathbf{P}_1$, $\mathbf{g}$ such that the condition of having both the final momentum vectors of the collision partners lie outside the occupied sphere in momentum space is satisfied.

Before the evaluation of $\bar{\sigma}$ can be undertaken, an appropriate cross section must be chosen.

[7] R. Serber, private communication.

Since the problem of the mean free path is not the primary one in this paper and since it will be computed in another fashion in Section III the cross section will be taken here to be isotropic in the center of mass frame, i.e., $\sigma=\sigma_T/4\pi$, where σ_T is a total constant cross section. In the other calculation referred to, this crude assumption will be dropped.

A coordinate system appropriate for the calculation of $\bar{\sigma}$ is shown in Fig. 1. This computation of $\bar{\sigma}$ will be given in detail since most of the results may be directly applied to the angular distribution calculation (see Part B of this section). The construction for finding the allowed values of $\mathbf{P}_1$ such that for a given momentum transfer, $\mathbf{g}$, the target particle lies outside the occupied sphere after the collision is made as follows: Move a distance $\mathbf{g}$ from the filled momentum sphere parallel to $\mathbf{g}$ and draw a sphere of radius P with this point as center. The region above the auxiliary sphere and inside the original one defines the allowed values of $\mathbf{P}_1$ (see Fig. 1). The integrations over $\mathbf{P}_1$ are most easily carried out using a cylindrical coordinate system with center at $\mathbf{g}/2$ as shown. The limits on the $\mathbf{g}$ integration are forced by the δ-function appearing in the expression for $\bar{\sigma}$ together with the demand that $P_f>1$, i.e., that the projectile lie outside the filled region after the collision. They will be given explicitly below.

To proceed with the evaluation, all quantities

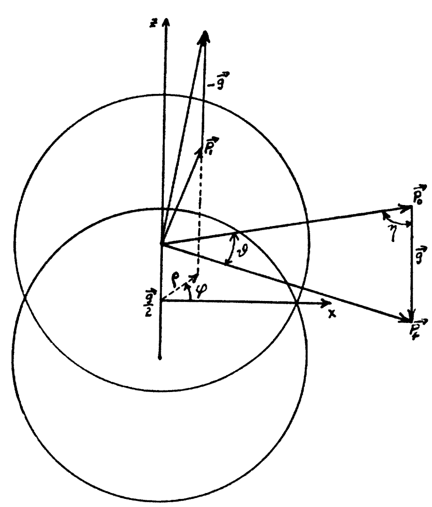

FIG. 1. Coordinate system used in computing the effective mean free path and the angular distribution of scattered particles.

must be expressed in terms of $\mathbf{g}$ and $\mathbf{P}_1$. The argument of the δ-function may be written in terms of the new variables ρ, z, φ by the use of the theorem

$$\delta(f(z)-0)=(\partial f/\partial z)^{-1}{}_{z=z_0}\delta(z-z_0), \tag{5}$$

where z_0 is the root of the equation $f(z_0)=0$. Using the relations $\mathbf{p}_f=\mathbf{p}_0+\mathbf{g}$ and $\mathbf{p}_0=|\mathbf{P}_0-\mathbf{P}_1|/2$, one finds easily

$$\begin{aligned} z_0&=-g/2+P_0\cos\eta,\\ (\partial f/\partial z)_{z=z_0}&=g/2P_0, \end{aligned}\tag{6}$$

where η is the complement of the angle between $\mathbf{g}$ and $\mathbf{P}_0$ (see Fig. 1). The fact that the contributing values of $\mathbf{P}_1$ lie on the plane $z=z_0$ is simply a statement of the physically obvious fact that the same specified momentum transfer parallel to $\mathbf{g}$ must be supplied by all target particles effective in scattering into $d\mathbf{g}$.

When every thing is written in terms of the above defined cylindrical coordinates, the z integration carried out, the expression for $\bar{\sigma}$ reduces to

$$\bar{\sigma}=\frac{N\sigma_T}{4\pi}\int d\mathbf{g}F(\mathbf{g}), \tag{7}$$

with

$$F(\mathbf{g})=\frac{3}{\pi g}\int_0^{2\pi}d\varphi\int_{\rho_1}^{\rho_2}\rho d\rho \tag{8}$$

where the constant density in momentum space has been inserted. The limits ρ_1, ρ_2 depend on the values g and $\cos\eta$. Three cases must be considered:

$$\begin{aligned} &(1)\quad g\leqslant 2, &0\leqslant z_0\leqslant 1-g/2,\\ &(2)\quad g\leqslant 2, &1-g/2\leqslant z_0\leqslant 1+g/2,\\ &(3)\quad g\geqslant 2, &g/2-1\leqslant z_0\leqslant g/2+1. \end{aligned}\tag{9}$$

The corresponding values of ρ_1, ρ_2 are

$$\begin{aligned} &(1) &\rho_1&=(1-P_0{}^2\cos^2\eta)^{\frac{1}{2}},\\ & &\rho_2&=(1-(g-P_0\cos\eta)^2)^{\frac{1}{2}},\\ &(2)\text{ and }(3) &\rho_1&=0\\ & &\rho_2&=(1-(g-P_0\cos\eta)^2)^{\frac{1}{2}}. \end{aligned}\tag{10}$$

The inequalities given in Eq. (9) completely define the region of integration in g, $\cos\eta$ space with the exception of the condition imposed by demanding that $P_f>1$. This yields the additional restriction

$$P_0-1\leqslant g\leqslant P_0+1,\ \cos\eta\leqslant(P_0{}^2+g^2-1)/2P_0g. \tag{11}$$

$F(\mathbf{g})$ may be evaluated trivially; the result is

Case (1)

$$F(\mathbf{g})=(3/P_0)(2P_0\cos\eta-g), \tag{12}$$

Cases (2) and (3)

$$F(\mathbf{g})=(3/P_0 g)\{1-(g-P_0\cos\eta)^2\}. \tag{13}$$

It is easy to see that $F(\mathbf{g})$ vanishes on the boundary lines $g=2P_0\cos\eta$, $g=P_0\cos\eta\pm 1$. The line $\cos\eta=1/P_0$ marks the transition from Case (1) to Cases (2) and (3) and is an explicit manifestation of the exclusion principle.

The remaining integration over $\mathbf{g}$ is trivial, although rather tedious. The result for $P_0 \geqslant \sqrt{2}$ is quite simple and is given by

$$\bar{\sigma}=N\sigma_T(1-7/5P_0^2). \tag{14}$$

The result for $P_0<\sqrt{2}$ is more complicated and will not be given. If the radius of the momentum sphere corresponds to 18 Mev, the potential well to 26 Mev, and the energy of the incident particle to 90 Mev outside the nucleus $\bar{\sigma}/N\sigma_T=0.78$. Assuming that the effective number of particles is 113 and the radius of the nucleus is 9×10^{-13} cm (corresponding to lead) and that the cross section σ_T is 0.064b (extrapolating the value of 0.083b at 90 Mev by a $1/E$ law) the mean free path is found to be 5.52×10^{-13} cm, whereas it would have been 4.3×10^{-13} cm with the neglect of the Pauli principle. It turns out that the isotropicity assumption underestimates the effect of the exclusion principle effect; the value of the effective cross section found in Section III, using a more realistic cross section, leads to a value of 6.20×10^{-13} cm.

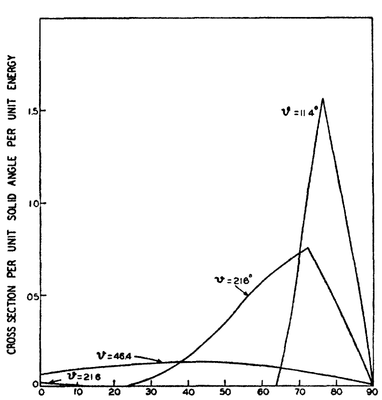

FIG. 2. Energy distribution of particles scattered from a heavy nucleus at fixed laboratory scattering angles. The energy of the incident neutron is 90 Mev. The discontinuous derivatives at the maxima result from the exclusion principle. The ordinate scale is in arbitrary units.

B. The Angular Distribution of Scattered Neutrons

The statistical model predicts that the angular distribution of neutrons scattered from a heavy nucleus will differ markedly from that expected qualitatively for high energy phenomena, namely, of strong forward scattering. Forward scattering implies small momentum transfers which, as was pointed out above, are very much reduced by the exclusion principle. Thus the angular distribution of scattered neutrons should show a pronounced dip in the forward direction. (Since the exclusion principle acts for the projectile, large momentum transfers are also discouraged, and there would be a corresponding dip in the backward direction.) It will be seen later that this is indeed the case. Another characteristic of the model is that for a fixed scattering angle there will be a distribution of energies among the scattered particles due to the motion of the target nucleons inside the nucleus.

The same assumption made in Part A of this section about having to deal with only one kind of particle will be made here. Two additional assumptions will be made: (a) The incident neutron makes only one collision inside the nucleus before escaping. This is not too good an assumption, as will be seen in Section III; however, the angular distribution is not greatly modified by the multiple collisions, as will be seen later. (b) The cross section for individual nucleon-nucleon collisions depends only on the momentum transfer involved in the collision. This point requires some discussion.

If one assumes that the Born approximation is valid, the cross section will be proportional to the square of a matrix element of the form

$$\langle \mathbf{p}_f | V | \mathbf{p}_0 \rangle=\alpha f_1(\mathbf{p}_0-\mathbf{p}_f)+\beta f_2(\mathbf{p}_0+\mathbf{p}_f),$$

where $\mathbf{p}_f$, $\mathbf{p}_0$ are the final and initial momenta, respectively, in the center of mass frame, and α, β are constants which depend on the particular sort of exchange and ordinary potential mixtures assumed. The general characteristic of the angular distributions associated with f_1 and f_2 are easily seen, since

$$f_1(\mathbf{p}_0-\mathbf{p}_f)\sim\int d\mathbf{r}e^{i/\hbar(\mathbf{P}_0-\mathbf{P}_f)\cdot\mathbf{r}}U_1(\mathbf{r}),$$

$$f_2(\mathbf{p}_0-\mathbf{p}_f)\sim\int d\mathbf{r}e^{-i/\hbar(\mathbf{P}_0+\mathbf{P}_f)\cdot\mathbf{r}}U_2(\mathbf{r}).$$

Evidently if the U's are reasonably well behaved f_1 will be large only when $\mathbf{p}_f\sim\mathbf{p}_0$ whereas f_2 will be large only when $\mathbf{p}_f\sim-\mathbf{p}_0$. Thus the angular distribution associated with f_1 is peaked in the forward direction, that of f_2 in the backward direction. As was pointed out at the beginning of this section, one would expect the effects of the exclusion principle to be prominent only in the case of very small or of very large momentum transfers. To see the effects, therefore, it will be sufficient to consider the case of small momentum transfer, in which case the most important contribution to be considered is that of the forward scattering, i.e., of $f_1(\mathbf{p}_0-\mathbf{p}_f)$. What shall be done in practice is to fit the experimentally measured neutron-proton angular distribution with a function $f_1(\mathbf{p}_0-\mathbf{p}_f)$ in the angular range of 0 to $\pi/2$ in the center of mass frame. It is, therefore, to be expected that the angular distribution in the heavy nucleus case will be correct only for angles somewhat less than $\pi/2$ in the laboratory frame since the transformation from the center of mass frame tends to concentrate the whole cross section in the forward direction. In Section III, the experimentally observed neutron proton cross section will be used.

The calculation proceeds exactly as that of $\bar{\sigma}$ in Part A, except that the integration over $\mathbf{g}$ is not carried out, since the differential effects are desired. Using the definition of $\mathbf{g}$ it is clear that $d\mathbf{g}=d\mathbf{P}_f$ where $\mathbf{P}_f$ is the final laboratory momentum of the scattered neutron. The cross section for scattering into $d\mathbf{P}_f$, namely, $\sigma_L d\mathbf{P}_f$, may be written as

Case (1)

$$\sigma_L d\mathbf{P}_f=\frac{3}{P_0}\sigma(\mathbf{p}_0-\mathbf{p}_f)\times\frac{P_0^2-P_f^2}{(P_0^2+P_f^2-2P_0P_f\cos\vartheta)^{\frac{1}{2}}}d\mathbf{P}_f, \quad (15)$$

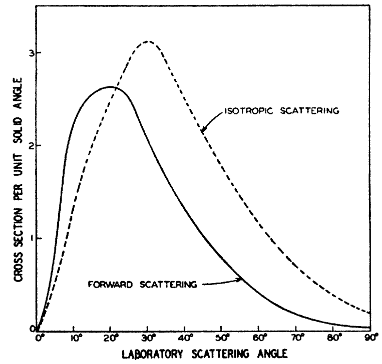

FIG. 3. Angular distribution of particles scattered by a heavy nucleus in the laboratory system assuming only a single collision inside the nucleus. The energy of the incident neutron is 90 Mev. Because of the symmetry of the neutron-proton scattering, these curves give also the distribution of recoil protons (see Section III). The ordinate scale is in arbitrary units and is not the same for the two curves.

Cases (2) and (3)

$$\sigma_L d\mathbf{P}_f=\frac{3}{P_0}\sigma(\mathbf{P}_0-\mathbf{P}_f)\times\frac{P_f^2-2P_fP_0\cos\vartheta+P_0^2P_f^2\sin^2\vartheta}{\{P_0^2+P_f^2-2P_0P_f\cos\vartheta\}^{\frac{3}{2}}}d\mathbf{P}_f, \quad (16)$$

where g and $\cos\eta$ in Eqs. (12) and (13) have been written in terms of (see Fig. 1) P_f and ϑ using

$$P_f^2=P_0^2+g^2-2P_0g\cos\eta,$$
$$g^2=P_0^2+P_f^2-2P_0P_f\cos\vartheta. \quad (17)$$

The regions of integration in P_f, $\cos\vartheta$ space follow in a straightforward fashion from Eq. (9), but the results are very complicated and will not be given. There is one modification of the region. The value of P_f must be greater than $(V_0)^{\frac{1}{2}}$ in order that the neutron be able to escape from the nucleus after suffering its collision.

The cross section chosen to fit the angular distribution in the region 0 to $\pi/2$ in the center of mass frame of neutron proton scattering at 90 Mev is

$$\sigma(\mathbf{p}_0-\mathbf{p}_f)=(\text{constant})/\{1.0714+(\mathbf{p}_0-\mathbf{p}_f)^2\}. \quad (18)$$

This cross section has no theoretical foundation and was taken only for simplicity of computation. The expressions for $\sigma_L d\mathbf{P}_f$ were evaluated for fixed values of the scattering angle ϑ, and the energy spectra of scattered neutrons was found. Then the angular distribution was calculated. As a numerical example, neutrons with an energy of 90 Mev outside the nucleus were chosen. The results are given in Figs. 2 and 3. In Fig. 2 the energy spectra are shown, and in Fig. 3 the angular distributions are given, the isotropic cross-section results being given for comparison. For lower energies the maximum in the angular distribution would occur at a larger angle because the particles would have to be deflected through larger angles in order to transfer the requisite amount of momentum in a given collision. A further discussion of these results will be given in Section IV.

In addition to the inelastically scattered neutrons treated above, there will also be some neutrons scattered with no change in energy. This is scattering by the nucleus as a whole and corresponds to the well-known diffraction scattering. The importance of this effect is that the elastic scattering is confined primarily to small angles and would thus tend to erase the dip predicted by the statistical model (Fig. 3). It will be seen later that this complication does not provide an insurmountable barrier to the experimental measurement of the decreased forward scattering of the inelastically scattered neutrons. Nevertheless, it seems worth while to estimate the effect semiquantitatively.

To the approximation in which the nucleus is regarded as a completely black sphere of radius a (sticking probability unity), the differential cross section may be easily calculated to be

$$\sigma d\Omega = a^2\left\{\frac{J_1(ka\vartheta)}{\vartheta}\right\}^2 d\Omega,^8 \qquad (19)$$

where J_1 is the Bessel function, k is the wave number of the incident neutron, and ϑ is the scattering angle. This result is valid for $\vartheta \ll 1$. If a is taken to be 9×10^{-13} cm and k corresponding to 90 Mev, the first minimum occurs at about 11°. The approximation of sticking probability unity is a good one, as may be seen from the results of Section III.

III. MORE DETAILED CALCULATIONS

The problem to be considered in this section is that of calculating in some detail quantities such as the energy delivered to the nucleus in bombardment by high energy neutrons, the number of collisions suffered by the projectile, the angular distribution of scattered particles taking into account multiple collisions and, finally, the mean free path of a nucleon passing through nuclear matter. The statistical model will again be used to describe the nucleus; however, more attention will be paid to the fact that both neutrons and protons are present. The experimentally observed neutron-proton scattering cross section will be used whenever possible.

The approach to these problems will be primarily a classical one in the sense that the concept of a definite trajectory for the particles will be used and also that of a definite radius for the nucleus. This is a well justified approximation since the wave-length divided by 2π of a nucleon with an energy of 90 Mev is about $\frac{1}{2}\times10^{-13}$ cm, or eighteen times smaller than the nuclear radius. The method to be used has been developed by S. Ulam and J. von Neumann.[9] The fundamental idea of the method is the following: One follows in detail, collision by collision, the passage of a large number of particles through the nucleus until the particles either escape or lose sufficient energy to be captured. Evidently, if a sufficiently large number were chosen, an exact solution to the problem would be obtained. Whenever it is necessary to make a choice of a number of equally probable events, this choice will be made by a random process. The method can be most easily explained by actually describing the successive steps involved in following a particle.

The first problem to be faced is that of how far the nucleon travels into the nucleus before making a collision. One imagines that the nucleon has penetrated the nucleus; as far as this nucleon is concerned it is immersed in an infinite medium of nuclear matter. The geometry of the sphere will be taken into account later. Then the total interval from zero to infinity is divided into regions of equal probability. Evidently the division is made according to the law

$$p = e^{-x/\lambda}, \qquad (20)$$

[8] H. Bethe and G. Placzek, Phys. Rev. **57**, 1075 (1940).

[9] S. Ulam and J. von Neumann, Bull. Am. Math. Soc. **53**, 1120 (1947).

where p is the probability of penetrating a distance x from the surface without suffering a collision, and λ is the mean free path *not* taking account the Pauli principle (the particle does not know if the collision is to be forbidden until it tries to collide). The path lengths are found to be $x_n = \lambda \ln 1/p_n$, where p_n designates which one of the equally likely intervals in which the collision has taken place and is given by n/N where N is the total number of divisions of the total interval from zero to one $(0 \leqslant n \leqslant N)$. The value of p_n is chosen at random and a path length is obtained.

The next decision to be made is that of the momentum of the struck target particle. The whole allowed region of momentum space is divided into regions of equal probability, i.e., equal volume. The number of these divisions should be sufficient to cover the region in a reasonable representative way. Since the probability of making a collision with a particle in the ith region is proportional to $p_{ri}\sigma(p_{ri})$ where p_{ri} is the relative momentum and $\sigma(p_{ri})$ is the total cross section for a collision with relative momentum p_{ri}, it is clear that the appropriate division into equal probability intervals is obtained by computing the partial sums

$$s_n = \sum_{i=1}^{n} p_{ri}\sigma(p_{ri}) \bigg/ \sum_{i=1}^{N_1} p_{ri}\sigma(p_{ri}),$$

where N_1 is the total number of divisions of the momentum space. Then a random number, m, between zero and one is chosen and if $s_n \leqslant m < s_{n+1}$ the collision is taken to be with a particle in region n.

Having decided on a collision partner, one must then find out the scattering angle. It is most convenient to work in the center of gravity system for this purpose. It is supposed that the differential cross section $\sigma(p_{ri},\vartheta)d\Omega$ is known. The appropriate values of ϑ_j are computed from

$$\frac{1}{\sigma(p_{ri})}\int_0^{\vartheta_j} \sigma(p_{ri},\vartheta)d\Omega = j/N_2, \qquad (21)$$

where $1 \leqslant j \leqslant N_2$ and N_2 is the total number of intervals chosen for division. The final vector momenta of the collision partners are determined from the conservation laws. Then one must see if the collision is permitted by the Pauli principle. If it is permitted, the whole procedure is repeated for the two final particles until they have escaped from the physical sphere or been captured. If the collision is forbidden, the particle is given a new path length along its original trajectory.

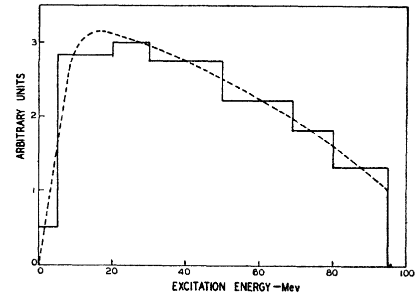

FIG. 4. Distribution of excitation energies of the residual nucleus immediately following the bombardment of a heavy nucleus by 86.6-Mev neutrons.

In the computations carried out in this paper, one hundred incident particles were followed. A greater number should, of course, be used, but if a greater number is chosen, the problem should be handled by a machine. The results obtained show some scattering but nevertheless indicate quite definite trends. The number of divisions used to obtain the path lengths was one thousand. The momentum sphere was divided into twenty regions and the scattering angles were divided into five regions from zero to $\pi/2$. The reason for going only to $\pi/2$ will be discussed immediately.

The choice of the differential cross section made here is based on the experimental fact that the neutron-proton scattering cross section is very nearly symmetric about $\pi/2$ in the center of mass system. This implies that the angular distribution of recoil protons is the same as that of the scattered neutrons. The convention was therefore made that only scattering angles less than $\pi/2$ in the center of mass frame would be considered; since targets and projectiles are treated on an equal footing, all possibilities are included. There is one important simplification resulting from this choice: Only one curve need be constructed for the determination of the scattering angles since the cross section may be chosen as a universal function of the momentum transfer, g, irrespective of the relative momentum

TABLE I. Results for 100 incident particles, of which 15 pass through the nucleus without collision. Energetics of the particles produced by the 85 which make successful collisions. All energies are in Mev.

No. particles emerging	No. of cases	Average excitation energy of residual nucleus	Average energy distribution of emerging particles decreasing energy 1	2	3
0	4	94.5			
1	58	41.6	45.0		
2	21	35.2	27.2	16.0	
3	2	40	14.5	9.5	6.5

$(g=\sqrt{2}p_r \sin\vartheta/2)$. It turns out that, on the basis of an interaction consisting of one-half ordinary forces and one-half exchange forces, which fits the experimental data,[7] the neutron-neutron scattering angular distribution has the same form as the neutron-proton; consequently the neglect of the difference between these types of collisions is justified. The exact form chosen is that given in Section II, Eq. (18). Further account of the presence of both neutrons and protons was taken by setting the minimum energy for escape from the nucleus at 14.5 Mev above the Fermi energy, an average between the neutron and proton barriers.

The energy dependence of the total cross section is taken to be inversely proportional to the relative energy, and the magnitude was fitted to the experimental result of 0.083b at 90 Mev. This has the consequence that $p_r\sigma(p_r)$ averaged over the momentum distribution is just $P_0\sigma(P_0)$, where P_0 is the projectile momentum, and provides a check on the method used to select the collision partners.

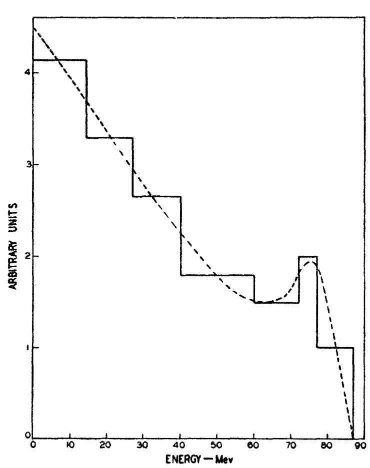

FIG. 5. Energy distribution of particles emerging at all angles immediately after the bombardment of a heavy nucleus by 86.6-Mev neutrons.

The actual calculations were carried out primarily by graphical means; analytical calculations would have required an exhorbitant amount of time if done with ordinary desk computing machines. The calculation described here required about two weeks full-time work by two people. The energy of the incident particles was taken to be 86.6 Mev, the depth of the potential hole to be 26 Mev, the maximum Fermi energy to be 18 Mev, and the nuclear radius to be 9.0×10^{-13} cm.

The mean excitation energy of the residual nucleus was found to be 42.5 Mev. The distribution of excitation energies is shown in Fig. 4; this curve represents 85 particles. The average number of collisions suffered by a particle escaping with more than 15 Mev is two, although about half the particles have only one collision. Note that these emerging particles may be target particles. The total energy distribution of all particles emerging at all angles is shown in Fig. 5; this curve represents 105 particles. The angular distribution of all emerging particles with energies greater than 15 Mev is shown in Fig. 6; this curve includes particles which have suffered up to five collisions before emerging and represents 76 particles. A further breakdown of the data is given in Table I. The effective cross section was found for particles with energies of 113 and 66 Mev inside the nucleus. The fractions of the total cross section at these energies are 0.69 and 0.32, respectively. It was found that 15 particles pass through the nucleus without a collision; an exact calculation based on a mean free path of 6.20×10^{-13} cm predicts 17 such events. It is interesting to note that the total cross section for lead found experimentally,[2] namely, 4.53b, agrees quite well with the value $0.85\times2\pi a^2$ which yields, with $a=9.0\times10^{-13}$, 4.32b. Of particles emerging with an energy greater than 15 Mev, 36 had suffered one collision, 29 had two collisions, eight had three collisions, five had four collisions, and one had five collisions. The intervals on the block diagrams were chosen so as to give a reasonably smooth curve and should not be regarded as giving a measure of the statistical accuracy involved.

Since each curve represents about 100 particles, the intervals on the diagrams represent from 10 to 15 particles.

IV. SUMMARY AND DISCUSSION OF RESULTS

(a) The theoretical angular distributions shown in Figs. 3 and 6 show that the expected dip in intensity in the forward direction for scattering high energy neutrons from heavy nuclei occurs over a relatively small angular interval; the interval is so small, about 25°, that experimental measurements will be difficult, although probably not impossible. It is interesting to note that the inclusion of multiple scattering does not radically change the angular distribution; this is due to the high number of single scatterings and to the fact that the double scatterings are strongly correlated to the single scatterings. The complication of the background of elastically scattered neutrons does not provide serious difficulty because of the fact that the distribution of recoil protons should be essentially the same as that of the scattered neutrons; one need, therefore, measure only the protons. In Fig. 2, the energy distribution of particles emerging at various angles is shown.

(b) The mean free path in nuclear matter for a neutron with energy 90 Mev outside the nucleus computed on the assumption of isotropic scattering in the center of mass system is 5.52×10^{-13} cm, whereas that computed using the observed angular dependence is 6.20×10^{-13} cm.

(c) The distribution of excitation energies of nuclei bombarded with 86.6-Mev neutrons is calculated (Fig. 4). The average excitation energy is 42.5 Mev. This energy will be distributed among the nucleons, and the subsequent behavior could be described by the evaporation model. The total energy distribution of emerging particles is shown in Fig. 5. The peak at the high energy end is believed to be real; it represents the large number of particles which suffer only one collision before escaping from the nucleus.

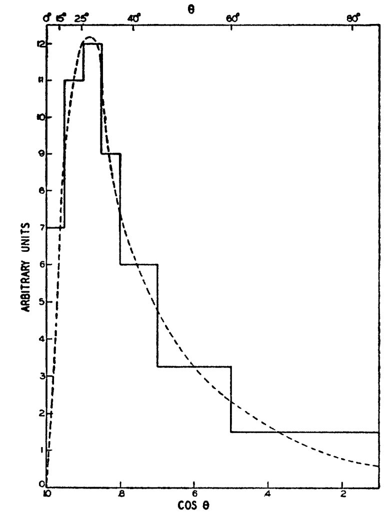

FIG. 6. Angular distribution of particles emerging from the nucleus taking into account multiple scattering (compare Fig. 3). The cosine of the laboratory scattering angle is given in the lower scale and the actual angle in the upper scale.

ACKNOWLEDGMENTS

The author wishes to express his gratitude to Dr. E. Fermi, who suggested this problem, for his frequent advice and encouragement. Thanks are also due G. F. Chew who shared the work in the tedious calculations and contributed essentially to all parts of this paper.